Analysis of anelastic dislocation effects in the presence of an unknown background

Ward L. Johnson
Materials Reliability Division, National Institute of Standards and Technology, 325 Broadway, Boulder, Colorado 80305, USA
(Received 7 May 2002; revised manuscript received 13 May 2003; published 12 August 2003)

The general problem of analyzing acoustic measurements of dislocation anelasticity in the presence of unknown background contributions is addressed for situations where material treatments induce changes in the physical parameters governing dislocation motion. The analytical approach focuses on the derivatives of the frequency-dependent acoustic damping and velocity with respect to a single experimental variable, such as irradiation flux, annealing time, or applied stress. The equation of dislocation motion is taken to be that of an overdamped harmonic oscillator with no restrictions on the specific physical model for the inertial, damping, and restoring parameters. The problem is simplified by considering all dislocations in a specimen to have the same values of these parameters, so that the contributions to the damping and velocity have the general form of Debye functions with a single relaxation time. Although the subsequent discussion remains focused on dislocations, the analytical approach is framed in such general terms that it can be applied to any relaxation or overdamped resonance having a Debye form. All possible combinations of changing relaxation strength and relaxation time are considered, and curves of the derivatives of the damping and velocity and the incremental exponents of the frequency dependence as a function of the product of the relaxation time and measurement frequency are presented. Since values for the abscissa in these plots cannot be directly measured in an experiment, additional practical curves are presented of the ratio of derivatives of the damping and velocity versus the measurable frequency exponents. For a given set of measurements, approximate values of physical parameters determined from inspection of these graphs can be used as initial guesses in a least-squares minimization to determine values of the relaxation time and the relative magnitude of changes in relaxation strength and relaxation time. Two examples of data from the published literature are used to illustrate the method of analysis.

DOI: 10.1103/PhysRevB.68.064108 PACS number(s): 62.40.+i, 61.72.Hh, 62.80.+f

I. INTRODUCTION

The analysis of anelastic effects (internal friction) in materials is usually complicated by the fact that a number of internal and external mechanisms dissipate acoustic energy. Since the goal of such measurements is to identify and characterize particular physical loss mechanisms through their dependence on frequency, temperature, or some other experimental variable, the contributions from other sources somehow must be removed from the analysis. In this paper, methods are presented for analyzing changes in the damping and velocity in material with changes in physical parameters that significantly affect only one anelastic contribution with a Debye dependence on frequency. Central elements of the analytical approach are expressed in very general terms, making them applicable to any mechanism with a Debye form, including point-defect and dielectric relaxations. However, the presentation is focused on measurements of dislocation anelasticity, because the problems of background subtraction generally seem to be most severe for such measurements. Part of the motivation for pursuing this work has been to provide a systematic approach for determining the validity of models for the recovery of damping and velocity in Al(Zn) (Ref. 1) and ferritic steels (Ref. 2) following the application of tensile loads.

In anelastic studies of point defects, extraction of the defect contribution can be relatively straightforward, because these contributions consist of one or more Debye functions (peaks in the damping and dispersions in the velocity as a function of temperature or frequency), each with an Arrhenius temperature dependence of the relaxation time. Because of the exponential dependence of the relaxation time on inverse temperature, point-defect damping peaks and velocity dispersions usually appear over relatively narrow temperature ranges and can be convincingly separated in an analysis by assuming a simple functional form for the temperature dependence of the background. A similar approach can sometimes be used with measurements as a function of frequency, if the relaxation time falls in an appropriate range. If the temperature dependence of point-defect relaxations is measured as a function of a material treatment, such as irradiation or annealing, the analysis can be even more straightforward. In this case, the relaxation times are usually constant—only the magnitude of the relaxations (proportional to the point-defect concentration) varies with material treatment—and the changes in damping and velocity are simply proportional to the Debye functions.

In studies of dislocations, the separation of anelastic contributions is usually much more challenging, because the relaxation time has a relatively weak temperature dependence with an unknown functional form. Complete characterization in the frequency domain has rarely been attempted because of the technical difficulties of performing accurate measurements over the necessary range of ultrasonic frequencies. The relaxation time, in addition to the relaxation strength, usually changes with material treatments, so that changes in damping and velocity are not simply proportional to the total dislocation contributions, as they are for point defects. For example, in the classical string model for dislocation anelasticity,[3,4] changes in pinning length affect both the re-

laxation time and relaxation strength. Irradiation has been effectively used to separate the dislocation contributions to internal friction, since it can provide values for the background damping (arising from sources other than dislocations) by essentially immobilizing dislocations with radiation-induced point defects. However, when performing many types of measurements, irradiation is not a feasible experimental procedure, and a direct determination of the background is not possible. Therefore, the general problem of analyzing dislocation effects in the presence of an unknown background has been a major impediment in this field of research. This paper seeks to address this problem.

II. DYNAMIC EQUATIONS

The equation of motion of a dislocation with Burgers-vector magnitude b under a resolved shear stress σ can be approximated as[5,6]

$$A\frac{d^2y}{dt^2}+B\frac{dy}{dt}+Ky=b\sigma, \tag{1}$$

where y is the displacement averaged over the length of the dislocation, A is an effective dislocation mass per unit length, B is the effective viscosity, and K is the restoring force.

The detailed physical model that is employed determines the dependence of A, B, and K on parameters of the dislocation and surrounding crystal. In the string model of Koehler[3] and Granato and Lücke,[4] A is on the order of ρb^2, where ρ is the density of the crystal. Taking the dominant first term in the Granato-Lücke[4] series expansion (that is, approximating the dislocation displacement as sinusoidal), K is equal to $\pi^2 C/L^2$, where C is the effective dislocation line tension and L is the distance between pinning points.[5,6] Granato and Lücke[4] approximate C as $2G_0b^2/[\pi(1-\nu)]$, where G_0 is the elastic modulus for shear in the glide plane with polarization parallel to the Burgers vector and ν is Poisson's ratio. Various physical mechanisms may contribute to B in the string model, including thermoelasticity, interactions with thermal phonons and electrons, and dragging of point defects.

Equation (1) is that of a damped forced harmonic oscillator. If $\sigma=\sigma_0\exp(i\omega t)$ (where σ_0 is a constant, ω is the angular frequency, and t is the time), then the solution is[7]

$$y=\frac{b\sigma_0}{A}\frac{\exp(i\omega t)}{\omega_0^2-\omega^2+iB\omega/A}, \tag{2}$$

where

$$\omega_0=\sqrt{K/A}. \tag{3}$$

The effect of dislocation motion on the propagation of acoustic waves is derived from the fact that the shear strain ϵ_d produced by the movement of a set of identical dislocations with density Λ is given by

$$\epsilon_d=\Lambda by. \tag{4}$$

If the acoustic wave has only a shear component with polarization parallel to the Burgers vector, the elastic strain of the surrounding lattice ϵ_e is equal to the ratio of the acoustic stress and the perfect-crystal elastic constant:

$$\epsilon_e=\sigma/G_0. \tag{5}$$

The more general case of arbitrary symmetries of the acoustic wave and dislocation is not considered here. This can be included by introducing an orientation factor in the final expression for the relaxation strength [Eq. (12), below].

The complex elastic compliance $J(\omega)$ of a crystal with dislocations is equal to the ratio of the total strain and stress:

$$\begin{aligned}J(\omega)&=\frac{\epsilon_e+\epsilon_d}{\sigma}\\&=\frac{1}{G_0}+\frac{\Lambda b^2}{A\omega_0^2}\frac{1-(\omega/\omega_0)^2}{[1-(\omega/\omega_0)^2]^2+[B/(A\omega_0)]^2(\omega/\omega_0)^2}\\&\quad-\frac{i\Lambda b^2}{A\omega_0^2}\frac{[B/(A\omega_0)](\omega/\omega_0)}{[1-(\omega/\omega_0)^2]^2+[B/(A\omega_0)]^2(\omega/\omega_0)^2}.\end{aligned} \tag{6}$$

The dislocation contributions to $J(\omega)$ are much smaller than the elastic contribution (first term), so that the fractional change in the absolute dynamic compliance[8] $|J(\omega)|$ relative to the perfect-crystal compliance J_0 ($\equiv 1/G_0$) is closely approximated by

$$\begin{aligned}\frac{|J(\omega)|-J_0}{J_0}&\approx\frac{J_{re}-J_0}{J_0}\\&=\frac{G_0\Lambda b^2}{A\omega_0^2}\\&\quad\times\frac{1-(\omega/\omega_0)^2}{[1-(\omega/\omega_0)^2]^2+[B/(A\omega_0)]^2(\omega/\omega_0)^2},\end{aligned} \tag{7}$$

where J_{re} is the real part of $J(\omega)$. The damping Q^{-1} is approximated by

$$\begin{aligned}Q^{-1}&\approx-\frac{J_{im}}{J_0}\\&=\frac{G_0\Lambda b^2}{A\omega_0^2}\frac{[B/(A\omega_0)](\omega/\omega_0)}{[1-(\omega/\omega_0)^2]^2+[B/(A\omega_0)]^2(\omega/\omega_0)^2},\end{aligned} \tag{8}$$

where J_{im} is the imaginary part of $J(\omega)$. The changes in the measured real elastic constant G and acoustic velocity v are given by

$$\frac{2(v-v_0)}{v_0}\approx\frac{|G|-G_0}{G_0}\approx-\frac{|J|-J_0}{J_0}, \tag{9}$$

where v_0 is the velocity in a perfect crystal.

In almost all experimental studies, dislocation motion is found to be overdamped. That is, $B/(A\omega_0) \gg 1$, and Q^{-1} and $(|G|-G_0)/G_0$ have significant magnitude only at frequencies much smaller than ω_0. In this case, $\omega/\omega_0 \ll 1$ at all frequencies of interest, and Eqs. (7)–(9) are closely approximated by Debye expressions,[8]

$$Q^{-1} \approx \Delta \frac{\omega\tau}{1+\omega^2\tau^2}, \tag{10}$$

$$\Phi \equiv \frac{v-v_0}{v_0} \approx -\frac{\Delta}{2}\frac{1}{1+\omega^2\tau^2}, \tag{11}$$

where

$$\Delta \equiv \frac{G_0\Lambda b^2}{A\omega_0^2} = \frac{G_0\Lambda b^2}{K}, \tag{12}$$

$$\tau \equiv \frac{B}{A\omega_0^2} = \frac{B}{K}. \tag{13}$$

The subsequent analysis presented here is restricted to this case. In addition, all dislocations in the specimen are approximated as having the same value of τ, so that the total dislocation contributions to Q^{-1} and Φ maintain the Debye form of Eqs. (10) and (11).

III. PROBLEM OF ANALYZING CHANGES IN Q^{-1} AND Φ

Suppose that acoustic measurements are performed as a function of a single experimental variable x, such as irradiation dose, time, or stress, which affects the anelastic behavior of dislocations in a specimen. Physical parameters affecting the dislocation dynamics vary with x, thus changing Δ and/or τ. If significant anelastic contributions from other sources are also present and the dependence of these contributions on x and ω is unknown, then the separate effect of x on the dislocation contributions to Q^{-1} or Φ obviously cannot be determined. On the other hand, if the contributions from sources other than dislocations are assumed, on the basis of physical arguments, to be independent of x, then information on the dislocation contribution can be extracted from the relative changes in Q^{-1} and/or Φ. In particular, if the dislocation contribution is assumed to have a Debye form [Eqs. (10) and (11)], then, in principle, approximate values of τ and Δ can be determined from a least-squares analysis of measurements of Q^{-1} and/or Φ at multiple frequencies performed at various values of x. Such an analysis is made much more complicated by the fact that the forms of the dependences of Δ and τ on x are generally unknown.

Under the assumption that anelastic contributions other than that of dislocations are independent of x, the damping has the approximate general form

$$Q^{-1}(\omega,x) \approx \Delta(x)\frac{\omega\tau(x)}{1+\omega^2\tau(x)^2} + C(\omega), \tag{14}$$

where $C(\omega)$ is unrelated to dislocations. If measurements are performed at two values of x, x_1 and x_2, then the difference in Q^{-1} is given by

$$\delta Q^{-1} \approx \Delta(x_2)\frac{\omega\tau(x_2)}{1+\omega^2\tau(x_2)^2} - \Delta(x_1)\frac{\omega\tau(x_1)}{1+\omega^2\tau(x_1)^2}. \tag{15}$$

This equation has four unknowns $\Delta(x_1)$, $\tau(x_1)$, $\Delta(x_2)$, and $\tau(x_2)$. Solutions for these unknowns can be obtained in a least-squares sense from measurements performed at four frequencies. Similarly, solutions can be obtained from measurements of velocity performed at four frequencies or from simultaneous measurements of damping and velocity performed at two frequencies. However, there are significant difficulties with such a direct approach. Equation (15) and the analogous equation for $\delta v/v_0$ are sufficiently complicated that relatively good initial guesses must be provided for the unknown parameters, and these are typically unattainable through physical arguments. Also, in some cases, broad ranges of values for the unknowns can provide nearly identical sums of square deviations in the fit, and valid solutions must be determined through consideration of constraints that can be fairly complicated when considering an entire set of measurements.

If measurements of both Q^{-1} and v at more than one frequency are available, a simplified analysis can be performed in terms of a reduced set of parameters associated with the derivatives of Q^{-1} and Φ with respect to x, which are approximated from discrete measurements. A method for doing this is presented in this paper. The results of such an analysis can provide initial guesses in a more complete direct analysis of discrete changes in the measured Q^{-1} [Eq. (15)] and v. The subject of this subsequent analysis is not discussed further in this paper.

In Sec. IV, dQ^{-1}/dx and $d\Phi/dx$ are expressed in terms of $\omega\tau$ and the derivatives of Δ and τ with respect to x. These expressions then are rewritten in terms of a new set of parameters, including a normalization factor η (dependent on Δ, $d\ln\Delta/dx$, and $d\ln\tau/dx$) and dimensionless parameters $\omega\tau$ and γ (a measure of the relative magnitudes of $d\ln\Delta/dx$ and $d\ln\tau/dx$). The normalized derivatives $\eta dQ^{-1}/dx$ and $\eta d\Phi/dx$ are plotted versus $\omega\tau$ for a number of values of γ spanning its range from -1 to 1. In Sec. V, the ratio of dQ^{-1}/dx and $d\Phi/dx$ (dependent only on γ, $\omega\tau$, and the sign of $d\Delta/dx$) is plotted versus $\omega\tau$. Also, the dependences of dQ^{-1}/dx and $d\Phi/dx$ on frequency are expressed in terms of logarithmic derivatives with respect to ω, and these are plotted versus $\omega\tau$. Finally, the ratio of dQ^{-1}/dx and $d\Phi/dx$ is plotted as a function of these frequency derivatives for various values of γ (by calculating values of the abscissa and ordinate for a sequence of values of $\omega\tau$). Since this last graphical representation employs measurable quantities for both the abscissa and ordinate, an approximate value for γ for given data can be determined from the plots, and earlier plots can then be used to determine the sign of $d\Delta/dx$ and estimates for $\omega\tau$ and η. This relatively coarse graphical es-

timation of parameters can be refined by a least-squares fit of the measurements to the general expressions for dQ^{-1}/dx and $d\Phi/dx$.

IV. DERIVATIVES OF DEBYE FUNCTIONS

Both Δ and τ in the Debye expressions [Eqs. (10) and (11)] may be dependent on the experimental variable x, so that the derivatives of Q^{-1} and Φ with respect to x are given by

$$\frac{dQ^{-1}}{dx} = \frac{d\Delta}{dx}\left[\frac{\omega\tau}{1+\omega^2\tau^2}\right] + \Delta\frac{d\tau}{dx}\frac{d}{d\tau}\left[\frac{\omega\tau}{1+\omega^2\tau^2}\right]$$
$$= \alpha\Delta\left[\frac{\omega\tau}{1+\omega^2\tau^2}\right] + \beta\Delta\left[\frac{\omega\tau}{1+\omega^2\tau^2} - \frac{2\omega^3\tau^3}{(1+\omega^2\tau^2)^2}\right], \tag{16}$$

$$\frac{d\Phi}{dx} = -\frac{1}{2}\frac{d\Delta}{dx}\left[\frac{1}{1+\omega^2\tau^2}\right] - \frac{\Delta}{2}\frac{d\tau}{dx}\frac{d}{d\tau}\left[\frac{1}{1+\omega^2\tau^2}\right]$$
$$= -\frac{\alpha\Delta}{2}\left[\frac{1}{1+\omega^2\tau^2}\right] + \beta\Delta\left[\frac{\omega^2\tau^2}{(1+\omega^2\tau^2)^2}\right], \tag{17}$$

where

$$\alpha \equiv \frac{1}{\Delta}\frac{d\Delta}{dx}, \tag{18}$$

$$\beta \equiv \frac{1}{\tau}\frac{d\tau}{dx}. \tag{19}$$

Measurements can be performed of the quantity $(1/v)(dv/dx)$, and, in essentially all situations, the anelastic contribution to v is sufficiently small that v can be replaced by v_0 in the prefactor to this expression. This measured quantity is, therefore, approximately equal to the derivative of Φ:

$$\frac{1}{v}\frac{dv}{dx} \approx \frac{1}{v_0}\frac{dv}{dx} = \frac{1}{v_0}\frac{d(v-v_0)}{dx} = \frac{d\Phi}{dx}. \tag{20}$$

At each point in an experiment, there are four unknown variables in Eqs. (16) and (17): Δ, α, β, and τ. However, since α and β are both multiplied by Δ in these equations, only three independent combinations of variables can be determined by a set of measurements. (Δ, α, and β cannot be separately determined through an analysis of dQ^{-1}/dx and $d\Phi/dx$.) Along with τ, the following combinations of variables are chosen:

$$\gamma \equiv \frac{\beta}{|\alpha|+|\beta|}, \tag{21}$$

$$\eta \equiv \frac{1}{\Delta(|\alpha|+|\beta|)}. \tag{22}$$

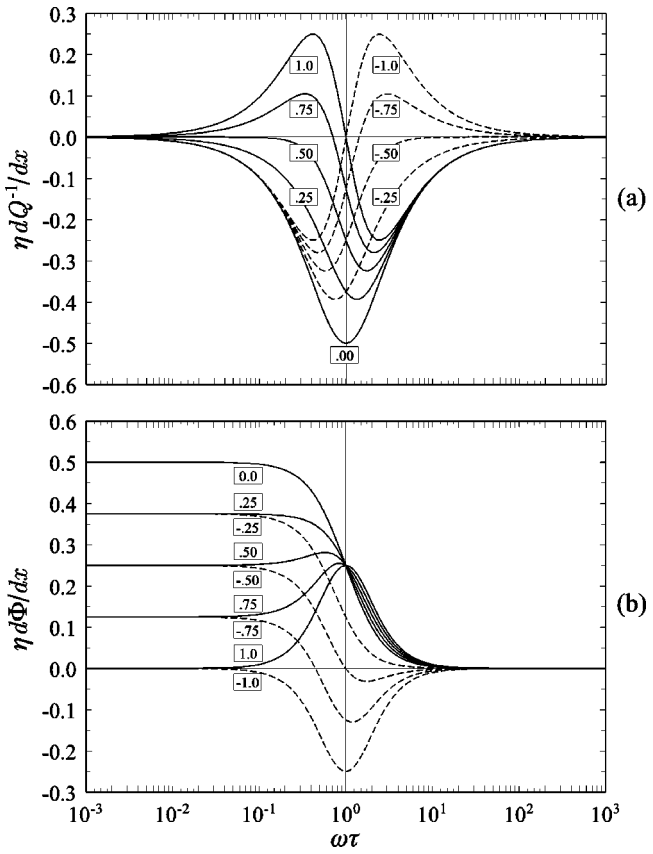

FIG. 1. The normalized derivative of the Debye functions plotted vs $\omega\tau$ for several values of γ with $\alpha \leqslant 0$. (a) $\eta dQ^{-1}/dx$ [Eq. (23)]. (b) $\eta d\Phi/dx$ [Eq. (24)]. Values of γ are indicated on the curves. Solid and dashed lines are used for $\gamma \geqslant 0$ and $\gamma < 0$, respectively. For $\alpha > 0$, the curves and values of γ are both reversed in sign.

An advantage of this choice for γ (relative to the simple ratio α/β) is that it has a finite range from -1 to $+1$. Equations (16) and (17) become

$$\eta\frac{dQ^{-1}}{dx} = [\gamma \pm (1-|\gamma|)]\frac{\omega\tau}{1+\omega^2\tau^2} - 2\gamma\frac{\omega^3\tau^3}{(1+\omega^2\tau^2)^2}, \tag{23}$$

$$\eta\frac{d\Phi}{dx} = \gamma\frac{\omega^2\tau^2}{(1+\omega^2\tau^2)^2} \pm \frac{|\gamma|-1}{2}\frac{1}{1+\omega^2\tau^2}, \tag{24}$$

where the plus sign applies for $\alpha > 0$ and the minus sign applies for $\alpha \leqslant 0$. These functions change sign when both α and γ change sign. That is, the functions for $\alpha < 0$ with a given γ are equal to the negative of the functions for $\alpha > 0$ with $-\gamma$. Therefore, characteristics of dQ^{-1}/dx and $d\Phi/dx$ can be explored by considering only $\alpha \leqslant 0$, which is perhaps the most commonly encountered case in experiments. The normalized derivatives with $\alpha \leqslant 0$ are plotted in Fig. 1 as a function of $\omega\tau$ for a series of values of γ from -1 to 1.

For $\gamma = 0$, the normalized derivatives shown in Fig. 1 are the Debye functions of Eqs. (10) and (11) divided by $-\Delta$. The simplest situation with $\gamma = 0$ has only the dislocation

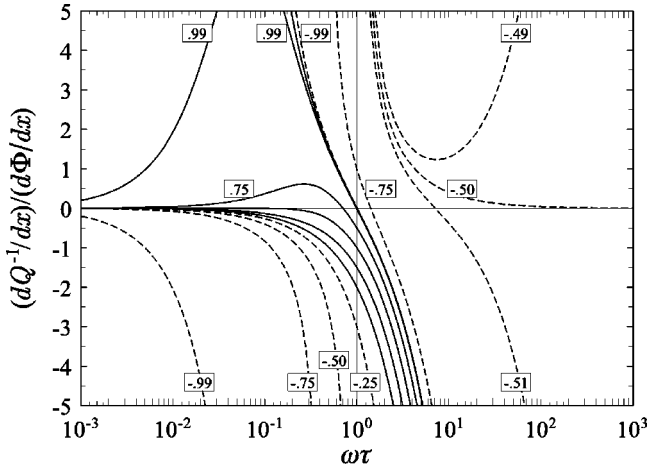

FIG. 2. The ratios of the derivatives, dQ^{-1}/dx and $d\Phi/dx$, plotted vs $\omega\tau$ for several values of γ with $\alpha \leqslant 0$. The curves are marked with the corresponding values of γ, except for the curves for $\gamma=0$, 0.25, and 0.50, which appear in sequence between $\gamma=-0.25$ and $\gamma=0.75$, and the curve for $\gamma=\pm 1$, which appears between $\gamma=0.99$ and $\gamma=-0.99$. Solid and dashed lines are used for $\gamma \geqslant 0$ and $\gamma<0$, respectively. For $\alpha>0$, the curves are unchanged, but the values of γ are reversed in sign.

density Λ dependent on x [Eqs. (12), (13), and (18)–(21)]. For $\gamma=-1$ and $\gamma=1$, all the x dependence resides in τ; this occurs if the viscosity B is the only changing physical parameter. The case with $\gamma=-0.5$ occurs when only K changes, so that the fractional changes in Δ and τ are equal (corresponding, in the string model, to only the pinning length L changing). Other values of γ correspond to more than one of the parameters Λ, B, and K changing with x [assuming that G and b in Eq. (12) are constant].

From Eqs. (23) and (24), solutions for the three variables γ, η, and τ can be determined at a particular point in an experiment (at a given value of x) by numerically fitting measurements performed at more than one frequency. That is, a least-squares minimization can be performed with ω as the independent variable, dQ^{-1}/dx and/or $d\Phi/dx$ as the dependent variables, and γ, η, and τ as adjustable parameters. Because of the powers of τ that appear in Eqs. (23) and (24), more than one solution for the three parameters may be found if only three measurements are used, so that additional measurements may be necessary to determine a unique solution. Some solutions are eliminated by the fact that γ must be real and that η and τ must be positive real.

V. GRAPHICAL DETERMINATION OF PHYSICAL PARAMETERS

In order to numerically fit measurements of dQ^{-1}/dx and $d\Phi/dx$, initial guesses must be determined for γ, η, and τ. A graphical determination of approximate values can be pursued by first taking the ratio of Eqs. (23) and (24) to obtain a single equation independent of η. In Fig. 2, this ratio $[(dQ^{-1}/dx)/(d\Phi/dx)]$ is plotted as a function of $\omega\tau$ for a series of values of γ with $\alpha \leqslant 0$. The curves for $\alpha \geqslant 0$ are the same, but the values of γ are reversed in sign. This figure, by

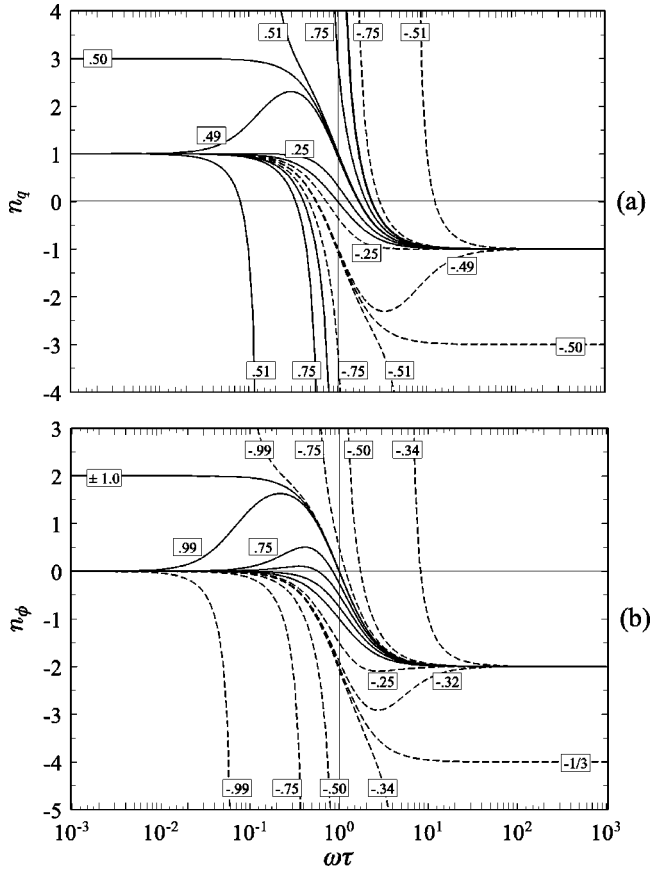

FIG. 3. The exponents of the frequency dependence for the derivatives of the Debye functions for several values of γ with $\alpha \leqslant 0$. (a) n_q [Eq. (28)]. (The unlabeled curve for $\gamma=0$ lies between the curves for $\gamma=-0.25$ and $\gamma=0.25$, and that for $\gamma=\pm 1$ lies between the curves for $\gamma=-0.75$ and $\gamma=0.75$.) (b) n_ϕ [Eq. (29)]. (The unlabeled curves for $\gamma=0$, 0.25, and 0.50 appear in sequence between those for $\gamma=-0.25$, and $\gamma=0.75$.) Solid and dashed lines are used for $\gamma \geqslant 0$ and $\gamma<0$, respectively. For $\alpha>0$, the curves are unchanged, but the values of γ are reversed in sign.

itself, cannot easily be used to analyze data, because $\omega\tau$ is not directly measurable.

In order to facilitate a nondimensional graphical representation in terms of measurable quantities, the frequency dependence is expressed in terms of the slopes of the curves of dQ^{-1}/dx and $d\Phi/dx$ versus $\omega\tau$. Over a sufficiently narrow range of ω, the absolute value of a well-behaved function $f(\omega)$ can be approximated by a straight line on a log-log scale:

$$\ln|f| \approx n \ln(\omega) + \ln A \tag{25}$$

or

$$|f| \approx A\omega^n. \tag{26}$$

Therefore, the exponent of the frequency dependence over this range is given by

$$n = \frac{d\ln|f|}{d\ln(\omega)} = \frac{\omega}{f}\frac{df}{d\omega}. \tag{27}$$

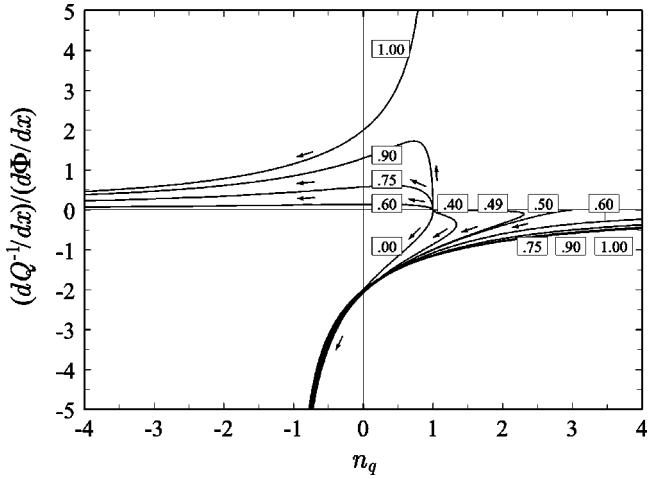

FIG. 4. The ratios of the derivatives, dQ^{-1}/dx and $d\Phi/dx$, plotted vs n_q for several values of positive γ with $\alpha \leqslant 0$. The curves are marked with the corresponding values of γ. The directions of increasing $\omega\tau$ are indicated by arrows. For $\alpha > 0$, the curves are unchanged, but the values of γ are reversed in sign.

The frequency exponents n_q and n_ϕ for the functions dQ^{-1}/dx and $d\Phi/dx$, respectively, are determined by inserting these functions [Eqs. (23) and (24)] into Eq. (27):

$$
\begin{aligned}
n_q &\equiv \frac{\omega}{(dQ^{-1}/dx)} \frac{d}{d\omega}\left[\frac{dQ^{-1}}{dx}\right] \\
&= \frac{\omega\tau}{(\eta dQ^{-1}/dx)} \frac{d}{d(\omega\tau)}\left[\frac{\eta dQ^{-1}}{dx}\right] \\
&= \frac{\omega\tau}{(\eta dQ^{-1}/dx)}\left[[\gamma \pm (1-|\gamma|)]\frac{1}{1+\omega^2\tau^2}\right. \\
&\quad \left. -[8\gamma \pm 2(1-|\gamma|)]\frac{\omega^2\tau^2}{(1+\omega^2\tau^2)^2} + 8\gamma\frac{\omega^4\tau^4}{(1+\omega^2\tau^2)^3}\right],
\end{aligned}
\tag{28}
$$

$$
\begin{aligned}
n_\phi &\equiv \frac{\omega}{(d\Phi/dx)} \frac{d}{d\omega}\left[\frac{d\Phi}{dx}\right] \\
&= \frac{\omega\tau}{(\eta d\Phi/dx)} \frac{d}{d(\omega\tau)}\left[\frac{\eta d\Phi}{dx}\right] \\
&= \frac{\omega\tau}{(\eta d\Phi/dx)}\left[[2\gamma \pm (1-|\gamma|)]\frac{\omega\tau}{(1+\omega^2\tau^2)^2}\right. \\
&\quad \left. -4\gamma\frac{\omega^3\tau^3}{(1+\omega^2\tau^2)^2}\right],
\end{aligned}
\tag{29}
$$

where, again, the plus sign applies for $\alpha > 0$ and the minus sign applies for $\alpha \leqslant 0$. Note that n_q and n_ϕ are independent of η (since $\eta dQ^{-1}/dx$ and $\eta d\Phi/dx$ are independent of η). The values of n_q and n_ϕ given by Eqs. (28) and (29) generally change during the course of an experiment, since γ and τ depend on the experimental variable x.

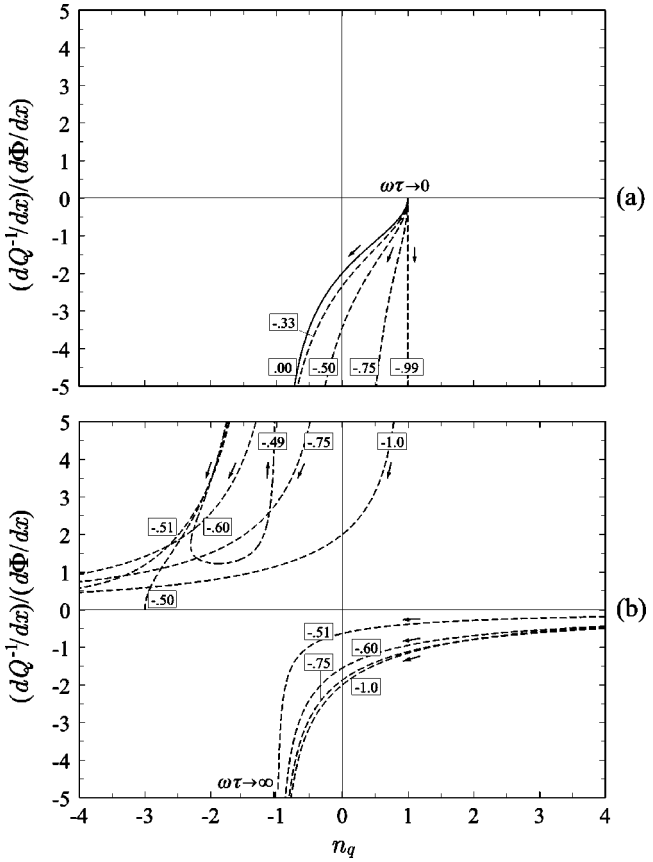

FIG. 5. The ratios of the derivatives, dQ^{-1}/dx and $d\Phi/dx$, plotted vs n_q for several values of negative γ with $\alpha \leqslant 0$. The curves are marked with the corresponding values of γ. The directions of increasing $\omega\tau$ are indicated by arrows. For $\alpha > 0$, the curves are unchanged, but the values of γ are reversed in sign.

Values calculated for n_q and n_ϕ for a series of values of γ with $\alpha \leqslant 0$ are plotted in Fig. 3 as a function of $\omega\tau$. Singularities in n_q and n_ϕ occur where dQ^{-1}/dx and $d\Phi/dx$, respectively, pass through zero. In the low- and high-frequency limits, dQ^{-1}/dx is proportional to ω and ω^{-1}, respectively, except for the case where $\gamma = \pm 0.5$. [In the limits of low frequencies with $\gamma = +0.5$ and high frequencies with $\gamma = -0.5$ the two terms involving $d\Delta/dx$ and $d\tau/dx$ in Eq. (23) cancel, making the frequency dependence stronger (ω^3 and ω^{-3}, respectively).] $d\Phi/dx$ is independent of frequency ($n_\phi = 0$) in the low-frequency limit, except for $\gamma = \pm 1$, and is proportional to ω^{-2} in the high-frequency limit, except for $\gamma = -1/3$.

The values of n_q or n_ϕ can be determined at a given point in an experiment from measurements at two frequencies. Therefore, a final graphical representation in terms of measurable quantities is obtained by eliminating the unknown $\omega\tau$ and plotting $(dQ^{-1}/dx)/(d\Phi/dx)$ versus n_q or n_ϕ with γ as the single unknown parameter, as shown in Figs. 4–7. The plots are generated by inserting a series of values of $\omega\tau$ into Eqs. (23), (24), (28), and (29). Arrows in the figures indicate the direction of increasing $\omega\tau$. The cases for $\gamma \geqslant 0$ and $\gamma \leqslant 0$ are plotted in separate figures. In addition, for both n_q and n_ϕ, the curves for $\gamma \leqslant 0$ are separated into two

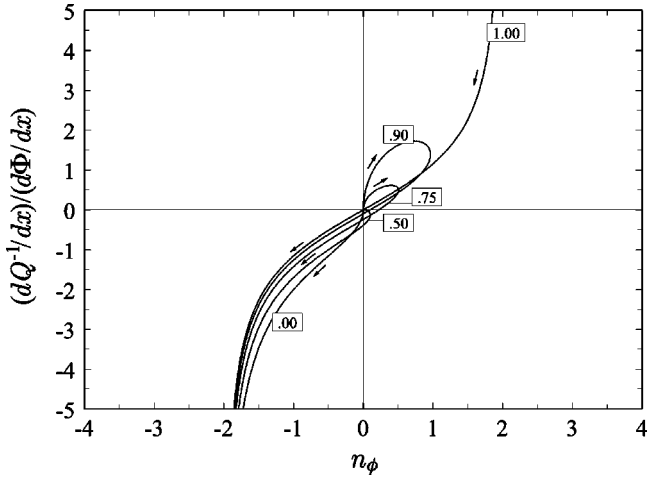

FIG. 6. The ratios of the derivatives, dQ^{-1}/dx and $d\Phi/dx$, plotted vs n_ϕ for several values of positive γ with $\alpha \leqslant 0$. The curves are marked with the corresponding values of γ. The directions of increasing $\omega\tau$ are indicated by arrows. For $\alpha > 0$, the curves are unchanged, but the values of γ are reversed in sign.

graphs (Figs. 5 and 7). To maintain consistency with previous figures, curves for $\gamma \geqslant 0$ are solid lines and those for $\gamma < 0$ are dashed lines.

$(dQ^{-1}/dx)/(d\Phi/dx)$, n_q, and n_ϕ are unchanged if both α and γ are reversed in sign. Therefore, the plots of n_q, and n_ϕ versus $\omega\tau$ (Fig. 3) and $(dQ^{-1}/dx)/(d\Phi/dx)$ versus n_q and n_ϕ (Figs. 4–7) are unchanged by a reversal of the sign of α, but the labels for γ are reversed in sign.

From an inspection of Figs. 4–7, one can find an approximate value of γ that yields the measured $(dQ^{-1}/dx)/(d\Phi/dx)$ with the measured n_q and n_ϕ simultaneously. Some care must be taken in such an analysis to make sure that the points determined for n_q and n_ϕ correspond to the same value of $\omega\tau$. To determine which sections of the curves correspond to the same $\omega\tau$ for positive γ, one must note the direction of increasing $\omega\tau$ on curves where there are two values of n_q or n_ϕ for a given value of $(dQ^{-1}/dx)/(d\Phi/dx)$. For example, with $\gamma = 0.90$ and $(dQ^{-1}/dx)/(d\Phi/dx)$ positive, $(dQ^{-1}/dx)/(d\Phi/dx)$ must be either increasing with $\omega\tau$ in both Fig. 4 and Fig. 6 or decreasing with $\omega\tau$ on both figures. For negative γ, the analysis is somewhat complicated by the fact that, for some values of γ, there are two ranges of $\omega\tau$ with negative $(dQ^{-1}/dx)/(d\Phi/dx)$. In this case, to ensure that comparisons are made between equivalent values of $\omega\tau$, one must use either Fig. 5(a) with Fig. 7(a) or Fig. 5(b) with Fig. 7(b). Having determined γ from an inspection of Figs. 4–7, one can determine $\omega\tau$ from Figs. 2 or 3 and, then, η from Fig. 1.

VI. EXAMPLE 1: HIKATA AND TRUELL

Thus far, few published acoustic studies of dislocation effects include measurements of dQ^{-1}/dx and $d\Phi/dx$ and the frequency dependence of both these quantities. One study that does include such information is that of Hikata and Truell,[9] which explores changes in attenuation and velocity in aluminum during plastic deformation. The measurements

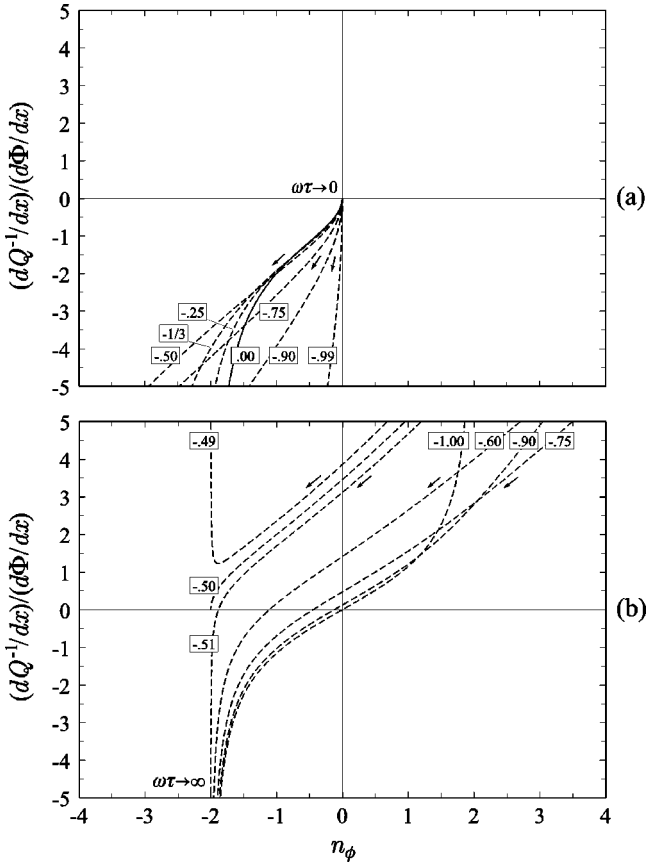

FIG. 7. The ratios of the derivatives, dQ^{-1}/dx and $d\Phi/dx$, plotted vs n_ϕ for several values of negative γ with $\alpha \leqslant 0$. The curves are marked with the corresponding values of γ. The directions of increasing $\omega\tau$ are indicated by arrows. For $\alpha > 0$, the curves are unchanged, but the values of γ are reversed in sign.

of Hikata and Truell as a function of plastic strain ϵ are shown in Fig. 8, with attenuation converted to Q^{-1} and fractional changes in v referenced to measurements at zero strain $[v(0)]$.

$d\Phi/d\epsilon$ is approximately equal to the derivative with respect to ϵ of the fractional changes in v referenced to $v(0)$:

$$\frac{d}{d\epsilon}\left[\frac{v(\epsilon)-v(0)}{v(0)}\right] = \frac{d}{d\epsilon}\left[\frac{v(\epsilon)-v_0}{v(0)}\right] \approx \frac{d}{d\epsilon}\left[\frac{v(\epsilon)-v_0}{v_0}\right] = \frac{d\Phi}{d\epsilon}. \tag{30}$$

This approximation rests on the normal assumption that anelastic effects on the velocity are relatively small, so that $v_0/v(0) \approx 1$ (where v_0, again, is the perfect-crystal velocity).

The dependence of Q^{-1} and v on strain is approximately linear up to a strain of approximately 8×10^{-4}. Linear regressions to the data in this range are shown in Fig. 8, except for the regression to $[v(\epsilon)-v(0)]/v(0)$ at 10 MHz, which, on the scale of the figure, is almost indistinguishable from that at 5 MHz. The slopes from these regressions and the corresponding frequency exponents are

$$\frac{dQ^{-1}}{d\epsilon}\Big|_{5\ \mathrm{MHz}} = 0.167 \pm 0.024, \tag{31a}$$

$$\frac{dQ^{-1}}{d\epsilon}\Big|_{10\ \mathrm{MHz}} = 0.463 \pm 0.032, \tag{31b}$$

$$\frac{d\Phi}{d\epsilon}\Big|_{5\ \mathrm{MHz}} = -8.71 \pm 0.67, \tag{31c}$$

$$\frac{d\Phi}{d\epsilon}\Big|_{10\ \mathrm{MHz}} = -7.5 \pm 1.1, \tag{31d}$$

$$n_q = 1.47 \pm 0.25, \tag{31e}$$

$$n_\phi = -0.21 \pm 0.31, \tag{31f}$$

$$\left(\frac{dQ^{-1}}{d\epsilon}\right) \Big/ \left(\frac{d\Phi}{d\epsilon}\right)\Big|_{5\ \mathrm{MHz}} = -1.92 \times 10^{-2} \pm 0.31 \times 10^{-2}, \tag{31g}$$

$$\left(\frac{dQ^{-1}}{d\epsilon}\right) \Big/ \left(\frac{d\Phi}{d\epsilon}\right)\Big|_{10\ \mathrm{MHz}} = -6.1 \times 10^{-2} \pm 1.0 \times 10^{-2}. \tag{31h}$$

Except for $d\Phi/d\epsilon$ at 10 MHz, the uncertainties listed for the slopes are simply the standard errors of the regressions, which may be smaller than the actual uncertainties in the data. Since only two points are included in the regression for $d\Phi/d\epsilon$ at 10 MHz, no standard error is produced by this regression analysis. The listed uncertainty in this case is estimated by assuming that each of the two points at 10 MHz has the same uncertainty as the standard error from the 5 MHz regression.

Under the assumption that α is negative, one can deduce a range of values for γ for the initial data of Hikata and Truell from an inspection of Figs. 4–7 (with $x \equiv \epsilon$). First, note that the plots of $(dQ^{-1}/dx)/(d\Phi/dx)$ versus n_q show only two possibilities with values within the margin of error of the measurements: (1) $0.40 < \gamma < 0.49$ (Fig. 4) and (2) $-0.51 < \gamma < -0.50$ [Fig. 5(b)]. The first of these possibilities is consistent with the measured n_ϕ (Fig. 6), but the second is not [Fig. 7(b)]. Therefore, if α is negative, γ must be between 0.40 and 0.49. If α is positive, γ must be between -0.40 and -0.49, since as described in the previous section, the values of γ labeling the plots in Figs. 4–7 are reversed in sign.

The sign of α can be determined from the plots of dQ^{-1}/dx versus $\omega\tau$ in Fig. 1(a). For $\alpha \leqslant 0$ [the case plotted in Fig. 1(a)] and $0.40 < \gamma < 0.49$, dQ^{-1}/dx is negative for all $\omega\tau$, which is contrary to the observed initial increase in Q^{-1}. Therefore, α must be positive, and γ must be between -0.40 and -0.49.

Having determined the range of possible γ, one can estimate $\omega\tau$ and η from Figs. 1–3. Figure 3 indicates that $\omega\tau$ must be between $\sim 8 \times 10^{-2}$ and $\sim 7 \times 10^{-1}$ to match the experimental value of 1.47 for n_q, and Fig. 2 indicates that it must be in the lower part of this range. Based on these ranges of values for γ and $\omega\tau$ and the measured $d\Phi/dx$ at 10 MHz [Eq. (31d)], η is determined, from Fig. 1, to be approximately 3×10^{-2}. Finally, with initial guesses within these ranges for γ, $\omega\tau$, and η, the best-fit values for γ, τ, and η are determined from a conjugate gradient minimization of the sum of the squared differences between the measured values for the derivatives $dQ^{-1}/d\epsilon$ and $d\Phi/d\epsilon$ at the two frequencies [Eqs. (31a)–(31d)] and the general expressions for the derivatives [Eqs. (23) and (24)]. In this minimization routine, the differences in $d\Phi/d\epsilon$ are multiplied by a factor equal to the average of the measured $(dQ^{-1}/d\epsilon)/(d\Phi/d\epsilon)$ at the two frequencies to provide approximately equal weighting of $dQ^{-1}/d\epsilon$ and $d\Phi/d\epsilon$. The final best-fit values are $\gamma = -0.474$, $\tau = 3.00 \times 10^{-9}$ s, and $\eta = 0.033$ which correspond to

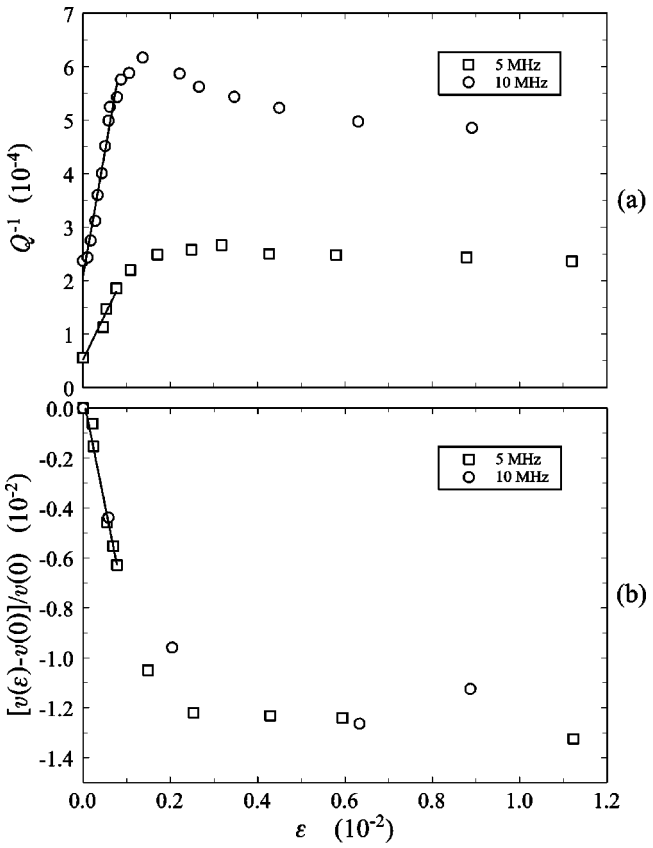

FIG. 8. Measurements by Hikata and Truell (Ref. 9) of Q^{-1} and fractional change in v as a function of plastic strain in aluminum. The changes in v are referenced to values measured at $\epsilon = 0$.

$$\frac{dQ^{-1}}{d\epsilon}\Big|_{5\ \mathrm{MHz}} = 0.169, \tag{32a}$$

$$\frac{dQ^{-1}}{d\epsilon}\Big|_{10\ \mathrm{MHz}} = 0.462, \tag{32b}$$

$$\frac{d\Phi}{d\epsilon}\Big|_{5\ \mathrm{MHz}} = -8.03, \tag{32c}$$

$$\frac{d\Phi}{d\epsilon}\Big|_{10\ \mathrm{MHz}} = -8.18. \tag{32d}$$

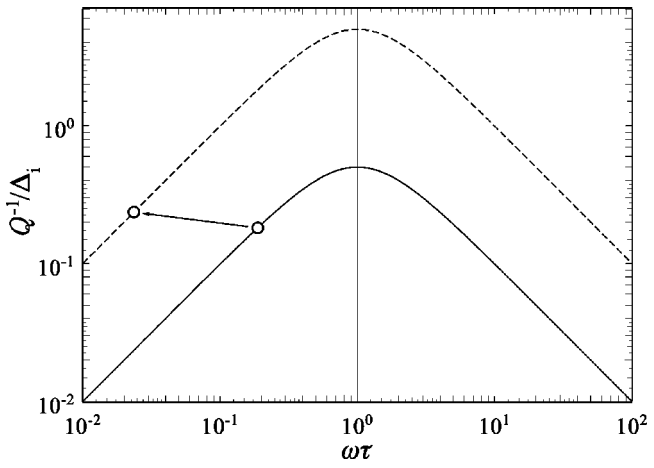

FIG. 9. The general situation resulting in changes in Q^{-1} as a function of ϵ during the measurements of Hikata and Truell (Ref. 9), deduced from an analysis of the initial slopes shown in Fig. 8. Solid curve: initial Q^{-1} vs $\omega\tau$ (at $\epsilon=0$), normalized to the initial relaxation strength Δ_i. The point marked on this curve corresponds to 10 MHz. Dashed curve: normalized Q^{-1} vs $\omega\tau$ at a value of ϵ that has induced a tenfold increase in Δ. The marked point again corresponds to 10 MHz.

These values of the derivatives lie within the ranges of the estimated uncertainties in the measured values [Eqs. (31a)–(31d)], except for $d\Phi/d\epsilon$ at 5 MHz, which is very slightly outside the range.

A value of γ near -0.5 is physically plausible. From Eqs. (12), (13), (18), (19), and (21), if $\gamma=-0.5$ and $\alpha>0$,

$$\frac{1}{K}\frac{dK}{d\epsilon}=\frac{1}{2}\frac{1}{\Lambda}\frac{d\Lambda}{d\epsilon}, \tag{33}$$

assuming that B, b, and G are constant. In the string model of Koehler[3] and Granato and Lücke,[4] K is inversely proportional to the square of the pinning length L (Sec. II), so that Eq. (33) becomes

$$\frac{1}{L}\frac{dL}{d\epsilon}=-\frac{1}{4}\frac{1}{\Lambda}\frac{d\Lambda}{d\epsilon}. \tag{34}$$

If the pinning length were determined entirely by dislocation network junctions, $(1/L)dL/d\epsilon$ would be equal to $-0.5(1/\Lambda)d\Lambda/d\epsilon$ (since, in this case, $\Lambda\propto L^{-2}$). On the other hand, if the pinning length were determined entirely by point defects, $(1/L)dL/d\epsilon$ would be positive, since the increase in Λ during deformation corresponds to a reduction in the total number of point defects per unit dislocation length and, also, dislocations break away from point defects during deformation. Therefore, since the results (with γ near -0.5) lie between these two extremes, L during the deformation is determined by a combination of pinning by network junctions and point defects with the network junctions being dominant [making $(1/L)dL/d\epsilon$ negative]. The fact that α is found to be positive simply indicates that the increasing Λ has a greater effect on Δ than the decreasing L.

Figure 9 shows the situation for Q^{-1} in the initial stage of deformation. The lower curve is Q^{-1} at $\epsilon=0$ normalized to the initial relaxation strength Δ_i and plotted versus $\omega\tau$ on a log-log scale [see Eq. (10)]. The point marked on this curve is at $\omega\tau=0.188$, the value for 10 MHz determined from the above analysis of slopes. The upper curve is Q^{-1} at a value of ϵ that has resulted in a tenfold increase Δ. If γ remains approximately constant at -0.474 (the value determined from the above analysis) during this process, then $\beta=-0.901\alpha$ [from Eq. (21)] and, from the definitions of α and β [Eqs. (18) and (19)],

$$\frac{d\ln\omega\tau}{d\epsilon}=-0.901\frac{d\ln\Delta}{d\epsilon}, \tag{35}$$

with ω constant. During the deformation that increases Δ by a factor of 10, $\omega\tau$ decreases to 0.024 (marked on the upper curve) and Q^{-1} at 10 MHz increases by 30%.

Since there appears to be considerable scatter in the measurements of v during the latter stages of deformation, no attempt is made here to perform a detailed analysis past the approximately linear region. However, assuming that Δ continues to increase and τ continues to decrease as deformation proceeds, one may note that the change in sign of the slope of Q^{-1} vs ε [Fig. 8(a)] can be explained only by γ decreasing below -0.50 [see Fig. 1(a) with dQ^{-1}/dx and γ reversed in sign]. Such a decrease in γ corresponds to the magnitude of $(1/\tau)d\tau/d\epsilon$ becoming greater than that of $(1/\Delta)d\Delta/d\epsilon$ or, within the framework of the string model, the rate of decrease of the pinning length becoming more significant relative to the increase of the dislocation density.

Hikata *et al.*[10] present qualitative conclusions about the dependence of Q^{-1} and v on ϵ that are consistent with the above analysis. They suggest that the increase in dislocation density during the initial stages of deformation causes the observed increase in Q^{-1} and decrease in v and that dislocation interaction forces at larger deformations impede the movement of dislocations and cause Q^{-1} to decrease after passing through a maximum.

VII. EXAMPLE 2: SIMPSON, SOSIN, AND JOHNSON

Measurements of Simpson, Sosin, and Johnson[11] can be used to illustrate an approach for a partial analysis of the derivatives of Q^{-1} and Φ in the absence of information on the frequency dependence. Simpson *et al.* found that, in several pure copper specimens, Φ increased monotonically and Q^{-1} displayed a peak as a function of electron irradiation. The results from one such specimen (E-3) are translated into the terminology of the current paper and shown in Fig. 10. The plotted values of Φ are equal to half the values of $\Delta E/E$ presented by Simpson *et al.* [see Eq. (9)] and are referenced to a specimen with a post-irradiation heat treatment that was assumed to produce nearly complete pinning of dislocations. Simpson *et al.* proposed that the peak in Q^{-1} could be explained by a point-defect drag mechanism determining the coefficient B, such that increasing numbers of irradiation defects caused $\omega\tau$ to rise above 1 (passing through the peak in the Debye function). Since this mechanism could not fully explain the changes in Φ, a second dislocation species with decreasing L was introduced into the model.

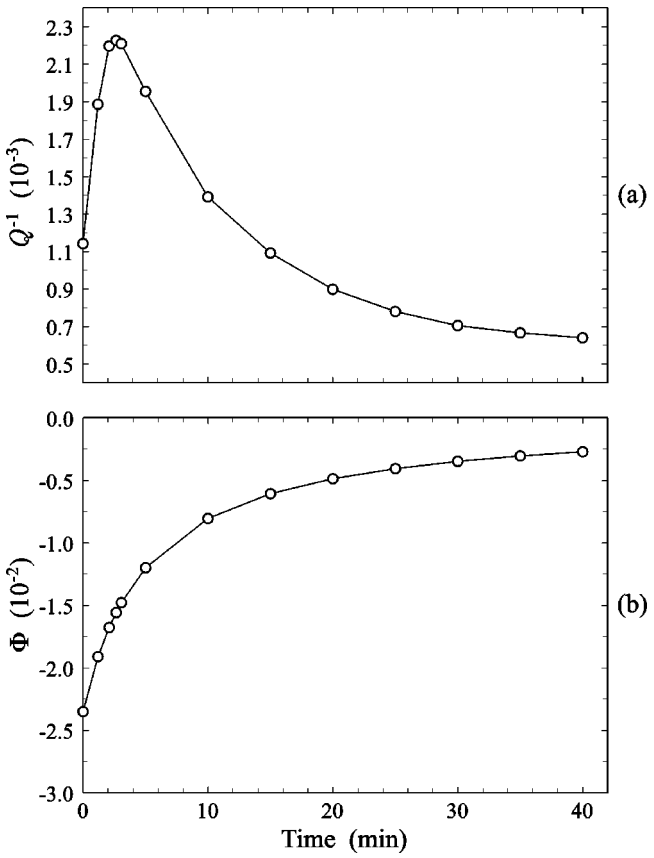

FIG. 10. Measurements by Simpson, Sosin, and Johnson (Ref. 11) of Q^{-1} and Φ as a function of irradiation time in pure copper (specimen E-3).

The interpretation provided by Simpson, Sosin, and Johnson for their results is disconcerting, considering that the measurement frequency was only 600 Hz and other studies[12,13] of pure copper have shown maxima in dislocation damping at much higher frequencies. Granato[5] suggested that the results can be explained with a single Debye relaxation having $\omega\tau \ll 1$ through the entire experiment, and he successfully analyzed some of the data considering both B and K to be dependent on the irradiation dose.

Analysis of the data of Fig. 10 using the expressions derived in Secs. IV and V is facilitated by first estimating the ratio $(dQ^{-1}/dt)/(d\Phi/dt)$ (Fig. 11). Since Simpson *et al.* performed measurements at only a single frequency, no information is available with respect to n_q or n_ϕ, and some assumption about the frequency regime must be made to proceed with the analysis. Considering that the frequency of the measurements is relatively low, one may assume that $\omega\tau \ll 1$ during the entire irradiation (although this assumption is at odds with the model of Simpson, Sosin, and Johnson). Under this assumption, the curves in Fig. 2 show that, for a single Debye function, a situation where $(dQ^{-1}/dt)/(d\Phi/dt)$ starts out positive and drops to a negative value (as in Fig. 11) will occur only if γ is initially greater than 0.5 and drops below 0.5 with radiation, assuming that $\alpha < 0$. The sign of α can be deduced by considering that the pinning length L is expected to decrease with an increase in radiation-induced point defects and the dislocation density Λ is expected to be constant. Therefore, Δ (proportional to L^2 in the string model) is expected to decrease with radiation, and this corresponds to $\alpha < 0$.

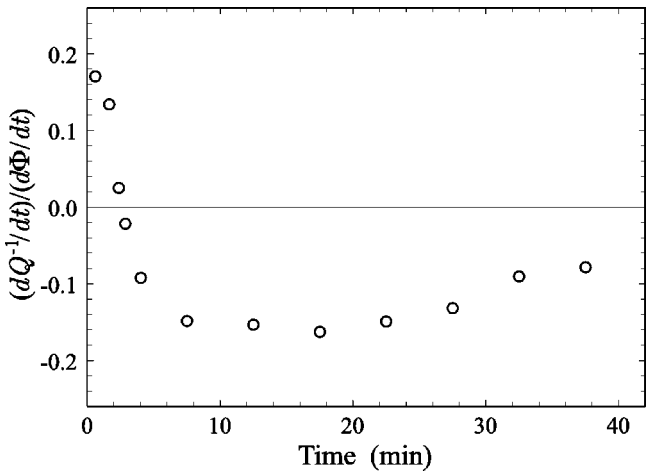

FIG. 11. The ratio of irradiation-induced changes in Q^{-1} and Φ in copper measured by Simpson, Sosin, and Johnson (Ref. 11) (specimen E-3), calculated from the discrete differences in the data points shown in Fig. 10.

In this scenario, τ increases with irradiation, since γ is positive [Eqs. (19) and (21)]. Although the relaxation strength decreases with radiation, τ initially increases enough that Q^{-1} at the measurement frequency increases. As irradiation proceeds, the changes in $\ln(\tau)$ become less than those of $\ln\Delta$, and Q^{-1} at the measurement frequency decreases. The peak in Q^{-1} corresponds to $\gamma = 0.5$.

Although the analysis of these data in terms of the derivatives of Q^{-1} and Φ serves to demonstrate the types of conclusions that can be made from limited measurements, this type of analysis may be unnecessary for this particular set of results. As mentioned above, Simpson, Sosin, and Johnson performed measurements on a specimen that they believed to have dislocations almost completely immobilized, and they used this as a reference for Φ. Since they also measured Q^{-1} for this reference specimen, this value can be subtracted from the Q^{-1} of other specimens during irradiation to separate the dislocation contributions from the background. Therefore, the Debye equations [Eqs. (10) and (11)] can be used to calculate $\omega\tau$ and Δ directly from the data:

$$\omega\tau = \frac{Q_d^{-1}}{2\Phi}, \tag{36a}$$

$$\Delta = -\frac{(2\Phi)^2 + (Q_d^{-1})^2}{2\Phi}, \tag{36b}$$

where Q_d^{-1} is the dislocation contribution to Q^{-1}. Granato[5] used these equations to analyze data from a different specimen of Simpson, Sosin, and Johnson and arrived at conclusions that are consistent with those obtained from the analysis of the derivatives presented here. A complete analysis of the data of Fig. 10 using Eq. (36) is beyond the scope of the current paper. However, it should be noted that values ob-

tained from Eq. (36a) confirm the assumption that $\omega\tau \ll 1$ throughout the course of the experiment.

VIII. CONCLUSION

Although acoustic measurements can be highly sensitive to anelastic dislocation effects, the analysis of such measurements often has been seriously impeded by an inability to separate dislocation effects from contributions arising from other sources of anelasticity or external damping. This problem is addressed in this paper for situations where changes in Q^{-1} and velocity occur as a function of some experimental variable that significantly affects only the contribution of dislocations to the anelasticity. The analytical approach assumes that both Q^{-1} and velocity are measured at two frequencies. It considers all possibilities for the ratio of fractional changes in the relaxation strength and relaxation time, and this introduces a variety of frequency-dependent curves for dQ^{-1}/dx and $d\Phi/dx$. By including all these possibilities, the discussion has gone beyond the most common approach of considering only changes in pinning length or dislocation density in the analysis of changes in dislocation anelasticity.

This formulation of the problem represents dislocations, with respect to their acoustic response, as overdamped oscillators with no specific physical model for A, B, or K in the equation of motion [Eq. (1)]. In addition to the string model of Koehler[3] and Granato and Lücke,[4] the approach is valid for models that describe the anelasticity of dislocations in terms of kink motion.

ACKNOWLEDGMENT

Dr. Andrew Granato provided many suggestions and comments that were very helpful in the development and presentation of this work.

[1] W. Johnson, Mater. Sci. Eng., A **309–310**, 69 (2001).
[2] W. Johnson, J. Alloys Compd. **310**, 423 (2000).
[3] J. S. Koehler, in *Imperfections in Nearly Perfect Crystals*, edited by W. Shockley, J. H. Holloman, R. Maurer, and F. Seitz (Wiley, New York, 1952), p. 197.
[4] A. Granato and K. Lücke, J. Appl. Phys. **27**, 583 (1956).
[5] A. V. Granato, in *Fundamental Aspects of Radiation Damage in Metals*, edited by M. T. Robinson and F. Y. Young, Jr. (National Technical Information Service, Springfield, VA, 1976), pp. 932–956.
[6] D. Lenz and K. Lücke, in *Internal Friction and Ultrasonic Attenuation in Crystalline Solids*, edited by D. Lenz and K. Lücke (Springer, New York, 1975), Vol. 2, p. 48.
[7] K. R. Symon, *Mechanics* (Addison-Wesley, Reading, MA, 1971), pp. 50–51.
[8] A. S. Nowick and B. S. Berry, *Anelastic Relaxation in Crystalline Solids* (Academic, New York, 1972).
[9] A. Hikata and R. Truell, J. Appl. Phys. **28**, 522 (1957).
[10] A. Hikata, R. Truell, A. Granato, B. Chick, and K. Lücke, J. Appl. Phys. **27**, 396 (1956).
[11] H.M. Simpson, A. Sosin, and D.F. Johnson, Phys. Rev. B **5**, 1393 (1972).
[12] G.A. Alers and D.O. Thompson, J. Appl. Phys. **32**, 283 (1961).
[13] R.M. Stern and A.V. Granato, Acta Metall. **10**, 358 (1962).